PROCEEDINGS OF SCIENCE

Polarization observables for Timelike Compton Scattering off the nucleon

Marie Boër*
Institut de Physique Nucléaire d'Orsay, CNRS-IN2P3, Université Paris-Sud, F-91406 Orsay, France.
E-mail: boer@ipno.in2p3.fr

Michel Guidal
Institut de Physique Nucléaire d'Orsay, CNRS-IN2P3, Université Paris-Sud, F-91406 Orsay, France.
E-mail: guidal@ipno.in2p3.fr

Marc Vanderhaeghen
Institut für Kernphysik, Johannes Gutenberg Universität, D-55099 Mainz, Germany.
E-mail: marcvdh@kph.uni-mainz.de

Deeply virtual exclusive processes of photo- and electro-production of photons and of mesons on the nucleon have been the subject of intense studies for the past ∼15 years. In such processes, a virtual photon is exchanged between a quark of the nucleon and a lepton. At sufficiently large photon virtuality, the scattering amplitude is factorized into a hard and a soft part. In this regime such reactions provide access to Generalized Parton Distributions (GPDs). These quantities contain informations about the longitudinal momentum and the transverse spatial distributions of quarks and gluons.

We will discuss our recent work on the hard exclusive process Timelike Compton Scattering (TCS), which corresponds to the reaction $\gamma N \to \gamma^* N \to e^+e^-N$. This reaction also involves the Bethe-Heitler process, where the final state e^+e^- pair comes from the the initial photon. We derived the amplitudes of these processes and we calculated, at typical JLab-12 GeV energies, all the single and double beam and/or target polarization observables off the proton and off the neutron.

XXIII International Workshop on Deep-Inelastic Scattering
27 April - May 1 2015
Dallas, Texas

*Speaker.

PoS(DIS2015)028

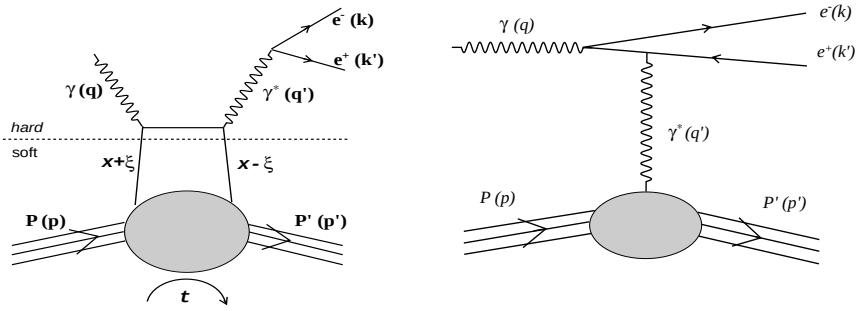

Figure 1: Left panel: the TCS handbag diagram at leading order and leading twist. Right panel: the BH diagram that interferes with TCS.

1. Introduction

Deeply virtual exclusive lepto- or photo-production processes on the nucleon provide access to its internal quarks and gluons structure. In particular, the Timelike Compton Scattering process (TCS, Fig. 1, left panel) corresponds to the scattering of a high energy real photon off a quark where a timelike virtual photon is emitted and decays into a lepton pair. TCS is measured in the reaction $\gamma N \to \ell^+\ell^- N'$. We will consider here only the case of an electron-position pair in the final state. It interferes with the Bethe-Heitler process (BH) where the incoming real photon splits into a lepton pair, that interacts with the nucleon (Fig. 1, right panel). At sufficiently large photon virtuality Q'^2 (where $Q'^2 = +q'^2 = (k+k')^2$), the TCS amplitude can be factorized into a hard perturbative scattering process, $\gamma q \to \gamma^* q'$, which can be calculated in a model-independant way via QED, and a soft part, corresponding to the non-perturvative QCD interactions in the nucleon. The soft part can be decomposed and parameterized by the Generalized Parton Distributions (GPDs) [1, 2, 3, 4, 5]. The GPDs are the Fourier transforms into momentum space of the QCD bilocal operators involved in the soft part of the amplitude. Without taking acount evolution effects (running in Q'^2), the GPDs depend on 3 independent variables, x, ξ and t, which represent respectively the longitudinal momentum fraction carried by the struck quark, the longitudinal momentum transfer to the quark (with $\xi \simeq \frac{Q'^2}{2s-Q'^2}$ for TCS on a fixed target) and the 4-momentum transfer squared $t = (p'-p)^2$. The squared momentum transfer t can be decomposed into a longitudinal and a transverse part, the latter corresponding to $\xi = 0$. It can be shown in a model independent way [6] that the Fourier transform of GPD$(x, \xi = 0, t)$ gives the probability to find a quark with momentum fraction x of the nucleon at a transverse distance $b_\perp$ of the center of the nucleon, where $b_\perp$ is the conjugate variable of t. At leading twist, the amplitude for massless quarks involves 4 chiral-even GPDs (without quark helicity flip) that are associated to 4 γ matrix structures: vector (GPD H), tensor (GPD E), axial (GPD $\tilde{H}$ and pseudo-scalar (GPD $\tilde{E}$).

The study in parallel of DVCS, where DVCS is the electroproduction of a real photon $\ell P \to \ell P \gamma$, and TCS is a promising way to access to the GPDs of the nucleon through two independent reactions. The DVCS has been studied for the past $\sim$ 15 years, both theoretically and experimentally (see Ref. [4] for a compilation of theoretical and experimental results) and first constraints and informations on the GPDs and nucleon imaging have been obtained. TCS has never been mea-

sured. As the DVCS and TCS leading twist and leading order amplitudes are complex conjugate [2], fitting both DVCS and TCS in parallel could lead to:
- a check of the GPD universality by comparing results from DVCS and from TCS,
- a better constrain of the system to constrain GPDs with fits, by fitting observables from both reactions at the same time,
- with a high enough level experimental precision, parallel fitting could allow for comparisons and study the higher twist and/or higher order structure of the amplitudes.

TCS was originally theoretically investigated in [7]. The TCS and BH unpolarized and circularly beam polarized cross sections were derived. The linearly beam polarized cross sections have been presented more recently in [8]. In our study, we calculated the BH and TCS amplitudes, where we waived some of the M^2/Q'^2 (where M is the proton mass) and t/Q'^2 approximations (twist 4 corrections) compared to the previous theoretical works. We also included twist 3 and twist 4 terms in order to restore the gauge invariance, as the twist 2 amplitudes are not gauge invariant. We studied the impact of these corrections on our results and found few percent deviations for the TCS cross sections and $< 1\%$ deviations for the spin asymmetries. We calculated all the unpolarized and beam and/or target polarized cross sections, with circularly or linearly polarized beam and with longitudinally or transversally polarized proton [9]. In this proceeding, we briefly summarize the formalism that we used and we present some of these results.

2. Formalism

TCS is studied through the reaction

$$\gamma(q)P \to \gamma^*(q')P'(p) \to e^-(k)e^+(k')P'(p'). \tag{2.1}$$

The outgoing photon has a large timelike virtuality, $Q'^2 \gg t$ to be in the factorization regime. From Deep Inelastic Scattering (DIS) and DVCS it is believed that $Q'^2 > 2$ GeV^2 and $-t < 1$ GeV^2 (or $\frac{-t}{Q'^2} < 0.1$). However, to be outside the mass range of meson resonances in the dilepton system, we restrict the study of TCS to the range 4 GeV^2 $< Q'^2 <$9 GeV^2.

We use a frame were the average photon momenta $\bar{q} = \frac{1}{2}(q+q')$ and proton momenta $P = \frac{1}{2}(P+P')$ are collinear along the $z-$axis and in opposite directions. We define the lightlike vectors along the positive and negative z directions as:

$$\begin{aligned} \tilde{p}^\mu &= P^+/\sqrt{2}(1,0,0,1), \\ n^\mu &= 1/P^+ \cdot 1/\sqrt{2}(1,0,0,-1), \end{aligned} \tag{2.2}$$

and we define the light-cone components $a^\pm$ by $a^\pm \equiv (a^0 \pm a^3)/\sqrt{2}$. The light cone momentum fractions x and ξ are defined respectively by $k^+ = xP^+$ and by $\Delta^+ = -2\xi P^+$ where $\Delta = (p'-p) = (q-q')$. In the asymptotic limit (neglecting terms in t/Q'^2), the variable ξ can be expressed as a function of Q'^2 and s, the squared center of mass energy, as $\xi = \frac{Q'^2}{2s-Q'^2}$. The results that we present in this proceeding are calculated for the asymptotic limit.

Using Ji's convention for GPDs [5], the TCS amplitude reads

$$T^{TCS} = -\frac{e^3}{q'^2}\,\bar{u}(k)\gamma^\nu v(k')\,\varepsilon^\mu(q)\,\Bigg[\tag{2.3}$$
$$\frac{1}{2}(-g_{\mu\nu})_\perp \int_{-1}^{1} dx \left(\frac{1}{x-\xi-i\varepsilon}+\frac{1}{x+\xi+i\varepsilon}\right)\left(H^n(x,\xi,t)\bar{u}(n')\,\not{n}u(n)+E^n(x,\xi,t)\bar{u}(n')i\sigma^{\alpha\beta}n_\alpha\frac{\Delta_\beta}{2M}u(n)\right)$$
$$-i(\varepsilon_{\nu\mu})_\perp \int_{-1}^{1} dx \left(\frac{1}{x-\xi-i\varepsilon}-\frac{1}{x+\xi+i\varepsilon}\right)\left(\tilde{H}^n(x,\xi,t)\bar{u}(n')\,\not{n}\gamma_5 u(n)+\tilde{E}^n(x,\xi,t)\bar{u}(n')\gamma_5\frac{\Delta.n}{2M}u(n)\right)\Bigg].$$

where we have used the metrics

$$\begin{aligned}(-g_{\mu\nu})_\perp &= -g_{\mu\nu}+\tilde{p}_\mu n_\nu+\tilde{p}_\nu n_\mu,\\ (\varepsilon_{\nu\mu})_\perp &= \varepsilon_{\nu\mu\alpha\beta}\,n^\alpha\tilde{p}^\beta.\end{aligned} \tag{2.4}$$

All results presented in the next section are calculated according to the VGG model for the GPDs parameterization [10, 11].

The BH amplitude reads

$$T^{BH} = -\frac{e^3}{\Delta^2}\,\bar{u}(p')\Gamma^\nu u(p)\;\varepsilon^\mu(q)\;\bar{u}(k)\;\left(\gamma_\mu\frac{\not{k}-\not{q}}{(k-q)^2}\gamma_\nu+\gamma_\nu\frac{\not{q}-\not{k}}{(q-k')^2}\gamma_\mu\right)v(k'), \tag{2.5}$$

with the virtual photon-proton electromagnetic vertex matrix

$$\Gamma^\nu = \gamma^\nu F_1(t)+\frac{i\sigma^{\nu\rho}\Delta_\rho}{2M}F_2(t). \tag{2.6}$$

The BH amplitude depends on the Dirac and Pauli form factors $F_1(t)$ and $F_2(t)$. For the proton form factors we used in this work the parameterization of [12, 13].

3. Results

3.1 Unpolarized cross section

The TCS+BH cross section depends on 4 independent kinematic variables, for fixed beam energy E_γ or ξ (with $E_\gamma = \frac{Q'^2}{4M(1+\xi)}$). We express it as a function of Q'^2 and t, and as a function of the lepton pair decay angles, in the e^+e^- center of mass frame, θ and ϕ that are presented on Fig. 2. We also express the linearly beam polarized spin asymmetries as a function of the angle Ψ, which corresponds to the angle between the reaction plane and the photon polarization vector. The unpolarized $\gamma P \to e^+e^-P'$ cross section at fixed beam energy is

$$\frac{d^4\sigma}{dQ'^2dtd\Omega} = \frac{1}{64\;(2\pi)^4\;(2ME_\gamma)^2}\;|T^{BH}+T^{TCS}|^2. \tag{3.1}$$

The $|T^{BH}+T^{TCS}|^2$ term is averaged over the proton and photon polarization and summed over the outgoing proton helicities. We display in Fig. 3 (left panel) the ϕ dependence of the unpolarized

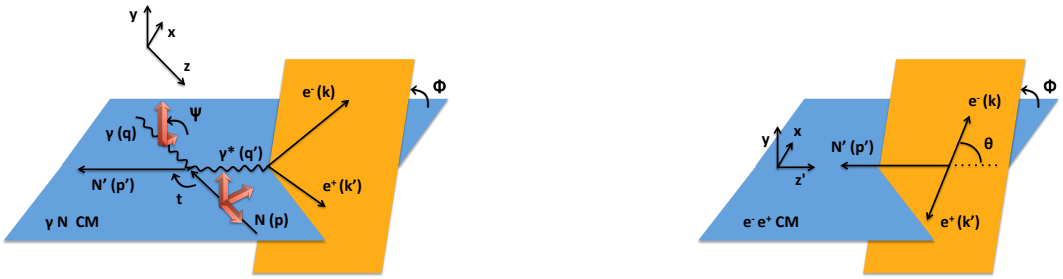

Figure 2: Left panel: scheme of the TCS reaction in the γP C.M.. The red arrows represent the 3 polarization states for the proton (along the x, y or z axis, where the xz plane is the reaction plane) and 2 polarization states for a linearly polarized photon (along $x-$ or $y-$axis). The angle between the beam polarization vector and the reaction plane is noted Ψ. Right panel: we boost the system and we define the 2 decay angles of the electron in the e^+e^- C.M., where θ and ϕ are respectively the polar and azimuthal angles with respect to the γP plane and the direction of the γ^* axis.

BH cross section, neglecting the TCS contribution, for three different values of θ. When $\theta \to 0$ or $\theta \to \pi$ we remark that one of the two BH diagrams strongly dominates and induces a peaks at, respectively $\phi = \pi$ or $\phi = 0$. This is due to the fact that, when the electron or the positron is collinear to the photon direction, all the particles are forced to be in the same plane. Away from these two singularities, at $\theta = \pi/2$, both BH diagrams have the same contribution to the total cross section, and we see (Fig. 3, left panel) only two small enhancements at $\phi = 0$ and $\phi = \pi$. The ϕ-shape for the TCS cross section is almost flat. The figure shows that the TCS cross section is suppressed by one to two orders of magnitude compared to the BH cross section. It can be generalized to most of the t and Q'^2 phase space [9]. Therefore, the TCS signal in the lepton pair photoproduction reaction shall be seen mostly through the interference with BH, that enhances it. When we include the TCS contribution to the cross section, we remark that the highest TCS/BH rate is obtained for $\theta = \pi/2$ (Fig. 3, right panel). Therefore, in order to maximize the counting rates in an experimental perspective, and at the same time staying far enough from the BH singularities, we integrate in the following the cross section over $\theta \in [\pi/4; 3\pi/4]$. The comparison between the two curves for the integrated cross sections of BH and of BH+TCS shows differences of a few percent, coming from the interference (Fig. 3, right panel).

3.2 Single and double spin asymmetries with a circularly polarized photon beam

The incoming photon beam can be circularly polarized or linearly polarized. At typical JLab 12 GeV kinematics, the circular polarization rate of the photon beam can reach 85% for the highest energy quasi-real photons (using a longitudinally polarized electron beam). We define the circularly polarized beam spin asymmetries (or single target spin asymmetries) as

$$A_{\odot U}\ (A_{Ui}) = \frac{\sigma^+ - \sigma^-}{\sigma^+ + \sigma^-}, \tag{3.2}$$

where the $\pm$ sign stands for left and right polarizations (or the direction of the target polarization along the i axis) and σ stands for the 4-differential cross section at fixed E_γ. We display the beam spin asymmetry as a function of ϕ in Fig. 4 (left panel). The fact that it cancels when we have

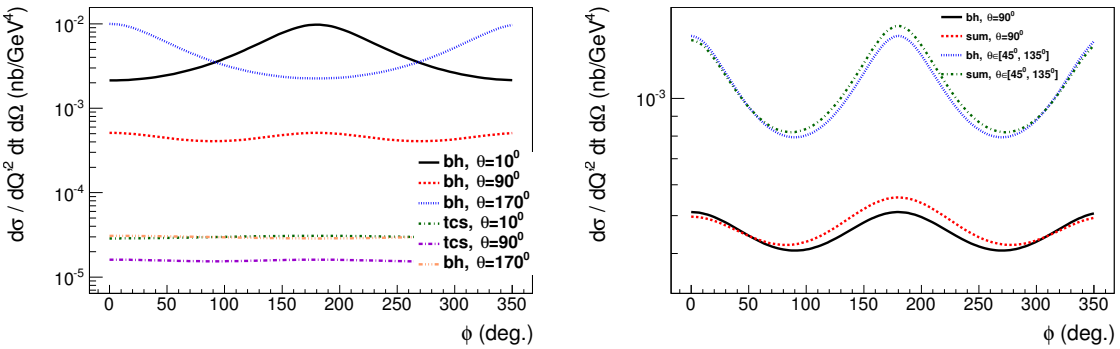

Figure 3: Left: unpolarized BH and TCS cross sections as a function of ϕ for various θ angles at $-t = .4$ GeV^2, $\xi = .2$ and $Q'^2 = 7$ GeV^2. Right: unpolarized BH and TCS+BH cross sections as a function of ϕ for $\theta = 90^\circ$ and for θ integrated over $[45^\circ; 135^\circ]$.

only the BH contribution reflects that it is proportionnal to the imaginary part of the amplitudes. Therefore, any non-zero asymmetry reflects the contribution from the TCS and allows the access to the imaginary part of the amplitudes. We display in Fig. 4 (top right panel) the circularly polarized beam spin asymmetry for $\phi = 90^\circ$ as a function of t. The different scenarii of GPD parameterization whithin the VGG model show the highest sensitivities of this observable to the H and the $\tilde{H}$ GPDs.

The target can be polarized along the proton direction (along the z-axis, in the γP C.M. frame, called longitudinal polarization), or transversally, along x and y axis, defined respectively as the axis perpendicular to the proton and in the reaction plane, or perpendicular to it. We display an example of a transversally polarized target spin asymmetries (along $x-$ axis) in Fig. 4 (bottom left panel). As these asymmetries are sensitive to the imaginary part of the amplitudes, the BH contribution cancels and they reflect the TCS strenght of the signal. The comparison between the different scenarii of GPD parameterizations shows a sensitivity to the H, $\tilde{H}$ and E GPDs.

We define the double spin asymmetries, with a circularly polarized photon beam as

$$A_{\odot i} = \frac{(\sigma_i^{++} + \sigma_i^{--}) - (\sigma_i^{+-} + \sigma_i^{-+})}{(\sigma_i^{++} + \sigma_i^{--} + \sigma_i^{+-} + \sigma_i^{-+})}, \tag{3.3}$$

where σ stands for the 4-differential polarized cross section, with a left or right photon polarization, denoted by the first $\pm$ superscript, and a polarized target, denoted by the index i and the second $\pm$ superscript (along the $x-, y-, z-$ axis). The circularly polarized beam-target double spin asymmetries are sensitive to the real part of the amplitudes. Fig. 4 (bottom right panel) presents such double spin asymmetries as a function of t for a transversally polarized target (along x-axis). The different curves show a strong sensitivity to the parameterization of the GPDs. However these asymmetries don't cancel for BH alone and it will require a good precision to evaluate the deviation coming from the TCS signal.

4. Conclusion

We presented a sample of our calculations of the unpolarized and single and double beam

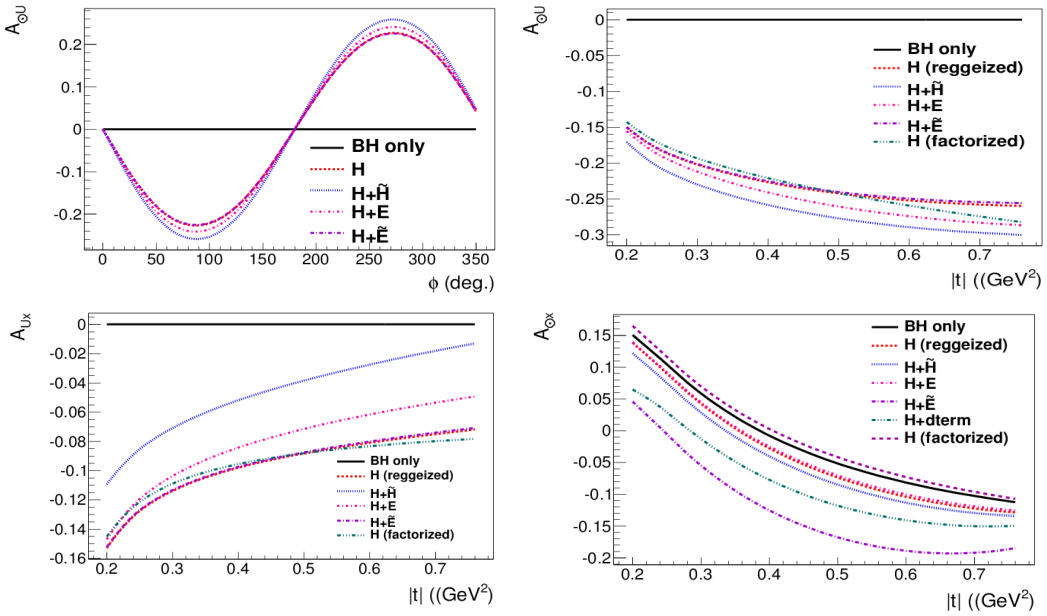

Figure 4: Single and double beam spin asymmetries for TCS+BH processes. Top left panel: $A_{\odot U}$ as a function of ϕ at $t = 0.4$ GeV^2. Top right panel: $A_{\odot U}(\phi = 90^\circ)$ as a function of $-t$. Bottom left panel: single target spin asymmetries as a function of t at $\phi = 90^\circ$ with a target polarization along the $x-$ axis. Bottom right panel: double spin asymmetry as a function of t at $\phi = 0^\circ$ with a transversally polarized target, along the $x-$axis, and a circularly polarized photon beam. Calculations have been performed at $Q'^2 = 7$ GeV^2, $\xi = 0.2$ and with θ integrated over $[\pi/4; 3\pi/4]$.

and/or target polarized cross sections and asymmetries for the TCS+BH reaction. We presented their t dependencies and discussed their sensitivities to the GPD parameterization ansatz.

References

[1] K. Goeke, M. V. Polyakov and M. Vanderhaeghen, Prog. Part. Nucl. Phys. **47**, 401 (2001).

[2] M. Diehl, Phys. Rept. **388**, 41 (2003).

[3] A.V. Belitsky, A.V. Radyushkin, Phys. Rept. **418**, 1 (2005).

[4] M. Guidal, H. Moutarde and M. Vanderhaeghen, Rept. Prog. Phys. **76**, 066202 (2013).

[5] X. Ji, Phys.Rev.Lett. **78**, 610 (1997); Phys.Rev.D **55**, 7114 (1997).

[6] M. Burkardt, Int. J. Mod. Phys. A **18** (2003) 173

[7] E. R. Berger, M. Diehl and B. Pire, Eur. Phys. J. C **23**, 675 (2002).

[8] A. T. Goritschnig, B. Pire and J. Wagner, Phys. Rev. D **89** (2014) 9, 094031

[9] M. Boër, M. Guidal and M. Vanderhaeghen, arXiv:1501.00270 [hep-ph].

[10] M. Vanderhaeghen, P.A.M. Guichon and M. Guidal, Phys. Rev. Lett. **80** 5064 (1998)

[11] M. Vanderhaeghen, P. A. M. Guichon and M. Guidal, Phys. Rev. D **60** 094017 (1999).

[12] O. Gayou *et al.* [Jefferson Lab Hall A Collaboration], Phys. Rev. Lett. **88** (2002) 092301

[13] E. J. Brash, A. Kozlov, S. Li and G. M. Huber, Phys. Rev. C **65** (2002) 051001